J Mol Model (2014) 20:2298
DOI 10.1007/s00894-014-2298-1

ORIGINAL PAPER

Rovibrational energy and spectroscopic constant calculations of $CH_4 \cdots CH_4$, $CH_4 \cdots H_2O$, $CH_4 \cdots CHF_3$, and $H_2O \cdots CHF_3$ dimers

Wiliam F. Cunha · Ricardo Gargano · Edgardo Garcia · José R. S. Politi · Alessandra F. Albernaz · João B. L. Martins

Received: 3 February 2014 / Accepted: 5 May 2014 / Published online: 18 June 2014

Abstract In this work, we performed a thorough investigation of potential energy curves, rovibrational spectra, and spectroscopic constants for dimers whose interactions are mediated by hydrogen bonds and other hydrogen interactions. Particularly, we deal with $CH_4 \cdots CH_4$, $CH_4 \cdots H_2O$, $CH_4 \cdots CHF_3$, and $H_2O \cdots CHF_3$ dimers by employing accurate electronic energy calculations with two different basis sets at the MP2 level of theory. Following this, the discrete variable representation method was applied to solve the nuclear Schrödinger equation, thus obtaining spectroscopic constants and rovibrational spectra. The harmonic constant, ω_e, presents a direct relation to the strength of dimer interactions. As a general rule, it was found that a decrease of interatomic distances is followed by the increase of D_e for all dimers. This behavior suggests that the interaction of $CH_4 \cdots CH_4$ is the weakest among all dimers, followed by $CH_4 \cdots CHF_3$, $CH_4 \cdots H_2O$ and the strongest interaction given by the $H_2O \cdots CHF_3$ dimer.

Keywords Dimers · Rovibrational spectra · Potential energy curve · MP2

Introduction

Noncovalent interactions are key factors to understanding many fundamental properties of chemical systems and processes. Despite being of much smaller magnitude when compared to covalent interactions, non-covalent phenomena are essential, for example, for the stability of biomolecules such as proteins [1] and nucleic acids [2] as well as for the physical-chemistry understanding of different environmentally important compounds [3, 4]. On the other hand, the description of this kind of interaction is known to require a great deal of resources, demanding sophisticated computational methods from both the level of theory applied and the basis set used [5]. A frequent procedure to overcome this difficulty is to use dimer calculations as a starting point in considering complex systems [6]. Additionally, determining intermolecular interactions experimentally show difficulties that reside at limited sampling and thermodynamic conditions to yield a potential energy surface [7]. Alternatively, intermolecular potentials are easily obtained through theoretical methods. Furthermore, the theoretical study of dimers consists of a standard technique in quantum chemistry and the properties that tend to alter their behavior are of fundamental importance in understanding many systems of technological interest.

Many researchers have investigated structural features of molecular clusters [8]. By studying the behavior of dimers, one can infer properties of larger clusters in an elegant and accurate fashion due to the possibility of applying computation of the highest level in small systems. Among these properties, the rovibrational spectra deserve special attention since a comparison between experimental and theoretical data consists on an unequivocal way to determine whether the performed calculation is suitable for each particular system [9, 10].

It is well known that the Coulombic term contribution plays a central role in the interaction energy of dimers, regardless the species considered. Thereupon, the behavior of dimers on which different kinds of multipole expansion moments primarily act has been extensively investigated in the last years [3, 4].

Of particular interest are those dimers originating from hydrogen bonding or another kind of hydrogen-mediated

This paper belongs to Topical Collection Brazilian Symposium of Theoretical Chemistry (SBQT2013)

W. F. Cunha · R. Gargano · A. F. Albernaz
Institute of Physics, University of Brasilia,
Brasilia 70919-970, Brazil

E. Garcia · J. R. S. Politi · J. B. L. Martins (✉)
Institute of Chemistry, University of Brasilia,
Brasilia 70919-904, Brazil
e-mail: lopes@unb.br

interaction. The chemistry of methane and water dimers, for instance, has received great attention, the former due to its importance as a powerful greenhouse gas and the latter for being a part of a number of biological phenomena. Greenhouse effects are also important in astrophysics, as the atmospheres on outer planets consist of mixtures containing methane. For example, the atmosphere of Titan (the largest moon of the planet Saturn) is composed of several percent of CH_4 and its greenhouse effect is widely studied [11–14]. Besides this effect, the recent awareness of highly concentrated methane trapped in the earth triggered many studies on methane hydrates or clathrates as a natural energy source [15]. Another molecule of special chemical interest is CHF_3, which is commonly used as solvent for supercritical fluid. This is the simplest representative molecule of the hydrofluorocarbon (HFCs) class, the common substitute of chlorofluorocarbons (CFCs). The interaction study of both heteromolecular and homomolecular dimers is of fundamental importance in understanding thermochemical properties.

An interesting fact on the mentioned species combination is that they have different Coulombic term contribution on the interaction energy: quadrupole–quadrupole ($CH_4 \cdots CH_4$), quadrupole–dipole ($CH_4 \cdots CHF_3$ and $CH_4 \cdots H_2O$) and dipole–dipole ($H_2O \cdots CHF_3$). In this sense, we have previously performed an extensive electronic structure investigation on energies, geometries, and some electrostatic properties for these systems, including basis set superposition error (BSSE) and zero point energy (ZPE)[16]. The goal was to obtain a good compromise between quality and computational cost by finding an optimal basis set and level of theory. Based on these previous results, the aim of this work is to calculate potential energy curves, rovibrational spectra, and spectroscopic constants. It is important to stress that, to the best of our knowledge, no experimental data is available for the spectroscopic constants and binding energies for most of the studied systems. Therefore, our work consists of an important contribution for comparing future data in the literature.

Rydberg expressions were used to fit the calculated data, thus obtaining a potential energy curve (PEC) for each system. The discrete variable representation (DVR) method was also used in order to obtain spectroscopic constants as well as the rovibrational spectra. Besides providing important data from the spectroscopic point of view, we also draw a comparison between the data arising from a simpler and a more sophisticated basis set. To accomplish this, we present two sets of results: one originated from aug-cc-pVDZ basis set, and the other from aug-cc-pVTZ, always considering the same level of theory—MP2—so that the comparison turns out to be consistent. The idea was to analyze the availability of the best method and basis set combination found previously to describe the dissociation profile, rovibrational energies, and spectroscopic constants.

The present work is organized as follows: in the Methodology section we present the methodology used in our calculations; our results together with their discussion are carried out in the Results and discussion section, and the main conclusions of the paper are reported in the Conclusions section.

Methods

Throughout this work, we performed a comparison between the results of calculations originating from two different basis sets. The goal is, in the spirit of the previous paper, to decide whether the use of an extended basis set is necessary to accurately obtain the desired properties. In order to do so, we considered the second-order Møller–Plesset perturbation theory (MP2) level of theory for calculating energies and electrostatic properties, and compared the results between basis sets aug-cc-pVDZ and aug-cc-pVTZ. The size difference (Table 1) of such basis sets is considerable, in such a way that the comparison between these bases is valuable. PECs were constructed starting from MP2/aug-cc-pVDZ and MP2/aug-cc-pVTZ-optimized dimer geometries as described in our previous paper[16]. The electronic structure calculations were carried out through MP2/aug-cc-pVDZ and MP2/aug-cc-pVTZ levels using the rigid SCAN and COUNTERPOISE keywords of Gaussian 09 [17] package in order to perform single point-type calculations for about 100 intermolecular distances. The obtained BSSE-corrected electronic energies were fitted into PEC analytical expressions, using the extended-Rydberg functions (ERF):

$$V_{ERF}(\rho) = -D_e\left(1 + \sum_k c_k \rho^k\right) exp(-c_1\rho) \tag{1}$$

where $\rho = R - R_e$ is the displacement from equilibrium distance (R_e), c_k's are adjustable parameters and D_e stands for the dissociation energy. All coefficients c_k were obtained through Powell's method [18]. Considering that the vibrational movement of the nuclei around the equilibrium position as approximately harmonic, the vibrational energies can be expanded near the point $\nu + \frac{1}{2}$. Analogous to the vibrational case, the rotational energies can be expanded near the point $j(j+1)$. The diatomic rovibrational energy equation is given by:

$$\varepsilon_{v,j} = \omega_e\left(\nu+\frac{1}{2}\right) - \omega_e x_e\left(\nu+\frac{1}{2}\right)^2 + \omega_e y_e\left(\nu+\frac{1}{2}\right)^3 + \ldots + \left[B_e + \alpha_e\left(\nu+\frac{1}{2}\right) - y_e\left(\nu+\frac{1}{2}\right)^2 + \ldots\right] j(j+1) + \ldots \tag{2}$$

Table 1 Size of the basis sets

Basis set	$CH_4 \cdots CH_4$	$CH_4 \cdots H_2O$	$CH_4 \cdots CHF_3$	$H_2O \cdots CHF_3$
aug-cc-pVDZ	118	100	160	142
aug-cc-pVTZ	276	230	345	299

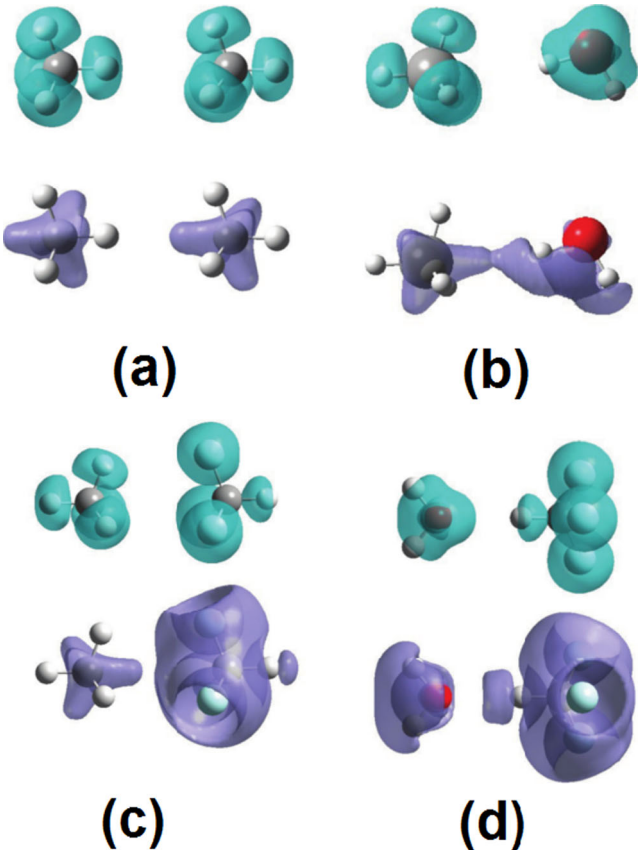

Fig. 1 Total electronic density difference MP2-HF at aug-cc-pVTZ for **a** $CH_4 \ldots CH_4$, **b** $CH_4 \ldots H_2O$, **c** $CH_4 \ldots CHF_3$, and **d** $H_2O \cdots CHF_3$

where ν and j are the vibrational and rotational quantum numbers, respectively. The coefficients of this expansion are called rovibrational spectroscopic constants. Also, $B_e iv \frac{h}{8\pi^2 c I_e}$, where I_e denotes the moment of inertia, c is the speed of light, and h is Planck's constant. Our approach was to evaluate the rovibrational spectroscopic constants by combining the rovibrational energies $E_{\nu,j}$ calculated from Schrödinger nuclear equation and Eq. (2), thus obtaining a "n" variables at "n" equation set system. It is important to remark that here Schrödinger nuclear equation is solved using the DVR method [19]. From this combination, spectroscopic constants can be derived as follows

$$\begin{aligned}
\omega_e &= \frac{1}{24}\left[14\left(\varepsilon_{1,0}-\varepsilon_{0,0}\right)-93\left(\varepsilon_{2,0}-\varepsilon_{0,0}\right)+23\left(\varepsilon_{3,0}-\varepsilon_{1,0}\right)\right] \\
\omega_e x_e &= \frac{1}{4}\left[13\left(\varepsilon_{1,0}-\varepsilon_{0,0}\right)-11\left(\varepsilon_{2,0}-\varepsilon_{0,0}\right)+3\left(\varepsilon_{3,0}-\varepsilon_{1,0}\right)\right] \\
\omega_e y_e &= \frac{1}{6}\left[3\left(\varepsilon_{1,0}-\varepsilon_{0,0}\right)-3\left(\varepsilon_{2,0}-\varepsilon_{0,0}\right)+\left(\varepsilon_{3,0}-\varepsilon_{1,0}\right)\right] \\
\alpha_e &= \frac{1}{8}\left[-12\left(\varepsilon_{1,1}-\varepsilon_{0,1}\right)+4\left(\varepsilon_{2,1}-\varepsilon_{0,1}\right)\right|+4\omega_e-23\omega_e y_e\Big] \\
\gamma_e &= \frac{1}{4}\left[-2\left(\varepsilon_{1,1}-\varepsilon_{0,1}\right)+\left(\varepsilon_{2,1}-\varepsilon_{0,1}\right)+2\omega_e x_e-9\omega_e y_e\right].
\end{aligned} \tag{3}$$

The rovibrational spectra follow straightforward from the solution of the Schrödinger nuclear equation with the correspondent PEC as potential through DVR method.

Results and discussion

In our previous work, an extensive investigation was performed on level of theory and basis set for calculations of energy, geometries, and electrostatic properties for $CH_4 \cdots CH_4$, $CH_4 \cdots H_2O$, $CH_4 \cdots CHF_3$, and $H_2O \cdots CHF_3$ dimers

Table 2 Fixed equilibrium distances (R_e) and dissociation energies (D_e) in the determination of the $CH_4 \cdots CH_4$, $CH_4 \cdots H_2O$, $CH_4 \cdots CHF_3$, and $H_2O \cdots CHF_3$ coefficients ck from the Rydberg potentials (Eq. 1) for aug-cc-pVDZ. *Values in parenthesis* are from the literature. References [20] and [21] are experimental values, while [22] is theoretical

Dimer	$CH_4 \cdots CH_4$	$CH_4 \cdots H_2O$	$CH_4 \cdots CHF_3$	$H_2O \cdots CHF_3$
ck	a_0^{-k}	a_0^{-k}	a_0^{-k}	a_0^{-k}
$c1$	$0.203382686907\times10^{-1}$	$0.230857686170\times10^{1}$	$0.361582776087\times10^{1}$	$0.237220288993\times10^{1}$
$c2$	$-3.22211794948\times10^{-1}$	$2.51257603628\times10^{-1}$	$0.398021865883\times10^{1}$	$0.127191496385\times10^{1}$
$c3$	$5.08247510799\times10^{-1}$	$-0.864093559465\times10^{-1}$	$0.282881511453\times10^{1}$	$-0.296604209444\times10^{-1}$
$c4$	$0.25295527071\times10^{-1}$	$-0.181040207405\times10^{-1}$	$0.149137285513\times10^{1}$	$-3.28895020224\times10^{-1}$
$c5$	$-1.55310384098\times10^{-1}$	$7.85383780995\times10^{-1}$	$7.63363127786\times10^{-1}$	$0.145901633852\times10^{1}$
$c6$	$1.4960793088\times10^{-1}$	$-0.853719043364\times10^{-1}$	$5.55549133750\times10^{-1}$	$1.05452396654\times10^{-1}$
$c7$	$-0.600836485497\times10^{-2}$	$-3.74360165973\times10^{-1}$	$2.51132794097\times10^{-1}$	$-8.17930679956\times10^{-1}$
$c8$	$0.134827425397\times10^{-1}$	$2.17507477212\times10^{-1}$	$-0.676312386267\times10^{-1}$	$4.39821924874\times10^{-1}$
$c9$	$-0.155418702112\times10^{-2}$	$-0.450409062488\times10^{-1}$	$-0.358294444093\times10^{-1}$	$-0.904450465643\times10^{-1}$
$c10$	$0.810918693618\times10^{-4}$	$0.331956925410\times10^{-2}$	$0.306243035295\times10^{-1}$	$0.702740548952\times10^{-2}$
R_e (Å)	4.2202 (4.2000)[20]	3.6237 (3.7024)[21]	3.9952	3.3943
D_e (Hartree)	0.000496538	0.00110272 (0.00161020)[22]	0.000757321	0.0054972
RMSD	7.56340494×10^{-7}	1.35221838×10^{-3}	3.04352994×10^{-6}	3.73487271×10^{-5}

Table 3 Fixed equilibrium distances (R_e) and dissociation energies (D_e) in the determination of the $CH_4\cdots CH_4$, $CH_4\cdots H_2O$, $CH_4\cdots CHF_3$, and $H_2O\cdots CHF_3$ coefficients c_k from the Rydberg potentials (Eq. 1) for aug-cc-pVTZ. *Values in parenthesis* are from the literature. References [20] and [21] are experimental values, while [22] is theoretical

Dimer	$CH_4\cdots CH_4$	$CH_4\cdots H_2O$	$CH_4\cdots CHF_3$	$H_2O\cdots CHF_3$
c_k	a_0^{-k}	a_0^{-k}	a_0^{-k}	a_0^{-k}
$c1$	$0.324278745477\times10^{1}$	$0.134875985565\times10^{1}$	$0.315243883642\times10^{1}$	$0.237661686609\times10^{1}$
$c2$	$0.275925159833\times10^{1}$	$-0.179977908317\times10^{1}$	$0.299680177303\times10^{1}$	$8.53309933561\times10^{-1}$
$c3$	$0.164360766311\times10^{1}$	$0.143620203804\times10^{1}$	$-3.45861365301\times10^{-1}$	$9.61684957869\times10^{-1}$
$c4$	$8.55298605268\times10^{-1}$	$-6.47373885595\times10^{-1}$	$-0.311335189897\times10^{1}$	$6.98455564955\times10^{-1}$
$c5$	$4.43486380482\times10^{-1}$	$1.60295223226\times10^{-1}$	$0.186937677273\times10^{1}$	$-2.87056958677\times10^{-1}$
$c6$	$1.52720803414\times10^{-1}$	$-0.698198059490\times10^{-2}$	$0.376838153830\times10^{1}$	$-2.22363695919\times10^{-1}$
$c7$	$-0.155004429505\times10^{-1}$	$-0.691460720547\times10^{-2}$	$-0.126519691381\times10^{1}$	$3.71008085864\times10^{-1}$
$c8$	$0.454213206620\times10^{-1}$	$0.189307691848\times10^{-4}$	$-0.109151872488\times10^{1}$	$-1.24547007831\times10^{-1}$
$c9$	$-0.811415555646\times10^{-2}$	$-0.204004593119\times10^{-3}$	$5.85706203455\times10^{-1}$	$0.150862825766\times10^{-1}$
$c10$	$0.320157983799\times10^{-2}$	$0.847000348691\times10^{-5}$	$-0.703863581585\times10^{-1}$	$-0.110298477080\times10^{-6}$
R_e (Å)	4.1152 (4.2000)[20]	3.5149 (3.7024)[21]	3.9887	3.2943
D_e (Hartree)	0.0005801885	0.00143501 (0.00161020)[22]	0.00090045	0.00572999
RMSD	1.58091367×10^{-6}	1.51344271×10^{-3}	2.32722458×10^{-6}	2.60461439×10^{-5}

[16]. The goal of this work [16] was to obtain the best possible compromise between accuracy and computational cost. For this, MPWB1K, PBE1PBE, MP2, and QCISD levels of theory were used with several basis sets. As the main result, we obtained that MP2/aug-cc-pVDZ was the best possible choice for geometry optimization procedures.

Therefore, in the present work, we have used the basis sets and method combinations that have proven to yield the best benefit–cost ratio for the static electronic properties in order to investigate the vibrational properties of each dimer, i.e., we used the MP2 method together with two different basis sets: aug-cc-pVDZ and aug-cc-pVTZ. The difference of the size between the two-basis set can be measured by the number of contracted basis functions used for each system, which bears a ratio of roughly in a 2:1 between aug-cc-pVTZ and aug-cc-pVDZ for all the considered systems[16]. This fact guarantees the comparison between a large and an intermediate basis set size.

The aug-cc-pVTZ basis set is considered of standard use in the literature, whereas our trial is to find out whether aug-cc-pVDZ yields the desired properties in good accordance to the former. In Fig. 1, the non-covalent interactions are of clear identification for all considered systems. We can infer a stronger intermolecular interaction for the hydrogen bonded systems, as it would be expected. The total electronic density difference plots are presented to stress the effects of including electron correlation on the dimer calculations, which is

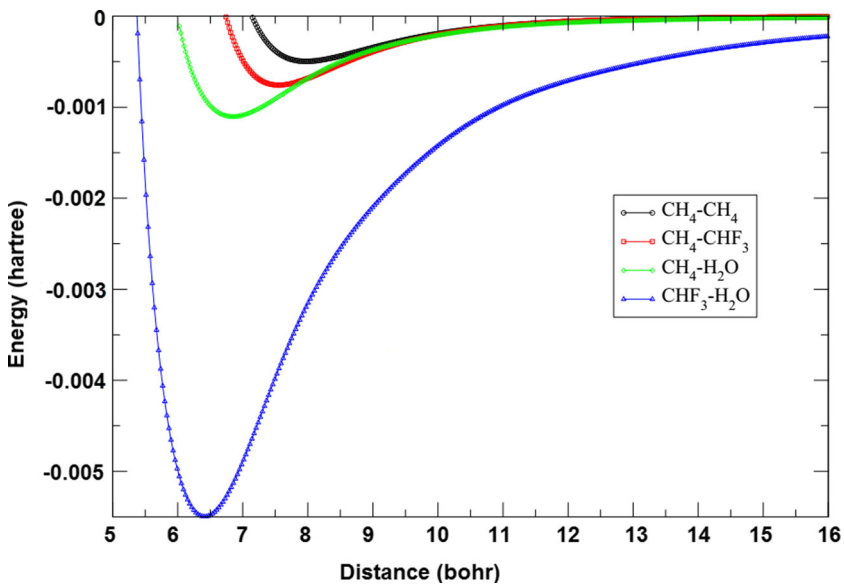

Fig. 2 Potential energy curve fittings on data obtained through 100 single points at MP2/aug-cc-pVDZ level

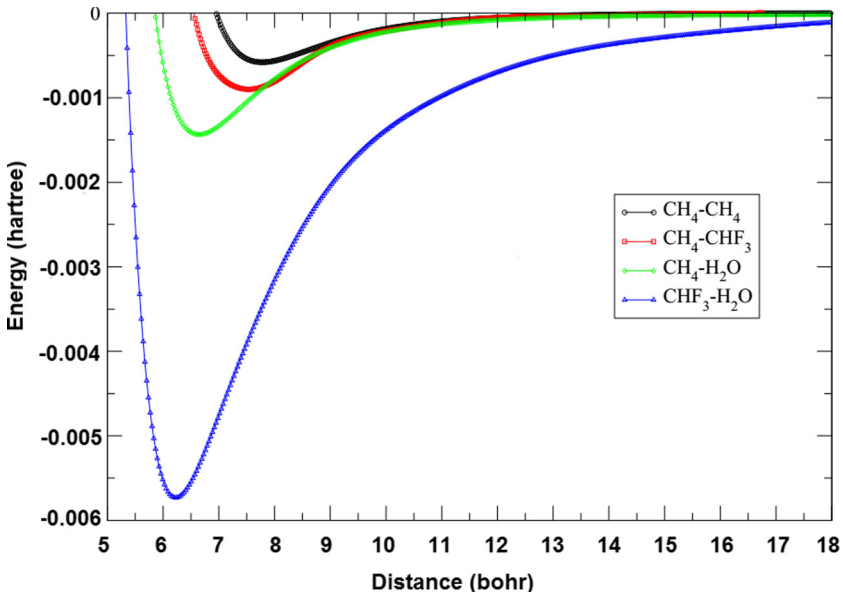

Fig. 3 Potential energy curve fittings on data obtained through 100 single points at MP2/aug-cc-pVTZ level

considered a good estimate for dispersion on molecular wavefunctions. This was achieved by subtracting Hartree–Fock total electron densities from MP2 ones on frozen geometries. Upper plots represent spatial regions with a decrease in electron density while lower plots represent the opposite. All surfaces in Fig. 1 were generated using the same isodensity value. The increase on electron density along the H ⋯ C intermolecular bond for $CH_4 \cdots CH_4$ dimer clearly shows that this dimer is stabilized mainly by dispersion interactions. It is observed that this pattern is repeated for all dimers, albeit in smaller proportion. At this point it is important to mitigate the possible misunderstanding led by our reasoning that dynamical correlation effects are mainly from dispersion. Moreover, we remark that the correlation effects, investigated through Fig. 1, are only an indication, although strong, of the dynamic dispersion and should not be accounted for the whole effect.

As a first step, we obtained the PEC for each dimer using both basis sets. This was carried out by considering each compound as geometrically frozen, then varying the intramolecular dimer distance, and finally computing the total electronic energy. Following this, we used a Rydberg expression to fit our data. The corresponding fitting coefficients and the root mean square deviation (RMSD) are listed in Table 2 for aug-cc-pVDZ and in Table 3, for aug-cc-pVTZ. We can note a systematic behavior of aug-cc-pVTZ presenting a slightly higher value of dissociating energy D_e compared to aug-cc-pVDZ. This can be attributed to the extra zeta addition in the former basis set, which in turn makes the calculation slower. Another evident feature is the decrease of equilibrium distances R_e from aug-cc-pVDZ to aug-cc-pVTZ. The small deviation from the corresponding fitting coefficients show that both basis sets yield satisfactory representations of the corresponding PEC for each dimer, thus, meaning that a simpler basis set is to be considered a practical choice in terms of PEC fitting.

In addition to the aforementioned agreement, our results find support from both experimental and theoretical previous works [16, 23–26]. Experimental comparison provides convincing evidence that our most stable geometry of $CH_4 \cdots CH_4$ dimer is in accordance with the methane cluster structure [27]. As presented in Tables 2 and 3, our equilibrium distance of $CH_4 \cdots CH_4$ dimer ($R_{C \ldots C}$) is about 4.2 Å, which agrees with established evidence [20]. Another remarkable agreement was found by studying dissociation energy from the same dimer, as can be seen in a recent work [28]. From an experimental point of view, an even more incisive result was achieved for the water methane dimer geometry, as we found an equilibrium distance of 3.6237 Å, whereas the

Table 4 Vibrational energies $\varepsilon - \nu, j=0$ in units of cm^{-1} for $CH_4 \cdots CH_4$, $CH_4 \ldots H_2O$, $CH_4 \ldots CHF_3$, and $H_2O \cdots CHF_3$ dimers with aug-cc-pVDZ

Line ν	$CH_4 \ldots CH_4$	$CH_4 \ldots H_2O$	$CH_4 \ldots CHF_3$	$H_2O \cdots CHF_3$
0	22.40183	32.95952	22.58717	46.48603
1	58.48035	91.88459	62.52315	137.60372
2	83.73141	140.05641	95.36321	225.69655
3	99.12863	176.72157	121.13111	310.17620
4	106.70051	203.34449	140.31300	390.45475
5		222.05535	153.55853	465.98511
6		233.23111	161.42677	536.31456
7		239.22125	165.70794	601.16165
8				660.50721
9				714.64936
10				764.14714
11				809.64440
12				851.68305
13				890.61276

Table 5 Vibrational energies $\varepsilon_{v,j=0}$ in units of cm^{-1} for $CH_4 \ldots CH_4$, $CH_4 \ldots H_2O$, $CH_4 \ldots CHF_3$, and $H_2O \ldots CHF_3$ dimers with aug-cc-pVTZ

ν	$CH_4 \cdots CH_4$	$CH_4 \cdots H_2O$	$CH_4 \cdots CHF_3$	$H_2O \cdots CHF_3$
0	24.77627	39.90570	22.40701	53.02176
1	65.68077	110.90651	66.19785	153.71463
2	95.20452	170.21528	106.37078	247.46297
3	114.06881	217.83500	138.98005	334.75919
4	124.02540	254.18852	161.30359	416.12416
5		280.15906	177.62427	492.04909
6		297.04473	189.54852	562.95017
7		306.72804	194.84768	629.14494
8		311.99826		690.84983
9				748.19334
10				801.24019
11				850.02488
12				894.59478
13				935.06034

experimental data suggest 3.7024 Å [21]. Another theoretical work dealing with this latter dimer showed dissociation energy with a deviation of around 0.1 kcal mol^{-1} from our results, a value which is to be considered negligible [22]. The consistency of these results yields confidence in the chosen simple combination of method and basis set.

The calculated points together with the fitted curves whose coefficients are listed in the previous tables are plotted in Figs. 2 and 3 for basis set aug-cc-pVDZ and aug-cc-pVTZ, respectively. We present the total energy in Hartrees against the inner dimer distance in Bohrs. Such curves represent different dimers that were put together for means of better comparison. From these figures, we can see the overall pattern of increasing D_e for all dimers from aug-cc-pVDZ to aug-cc-pVTZ. Also, the slight decrease in R_e can also be noted as a left shift of the curves from aug-cc-pVDZ to aug-cc-pVTZ.

Our next task is to investigate the vibrational energies for different vibrational states on each dimer and compare these results between both basis sets. Table 4 presents the summary of these calculations for basis set aug-cc-pVDZ, whereas Table 5 deals with the data arising from aug-cc-pVTZ. These energies were obtained by solving the nuclear Schrödinger equation considering ν varying between 0 and 13 for j=0.

The dimers reduced masses are equal to 14622.31541 $u.a.(CH_4 \cdots CH_4)$, 15469.08932 $u.a.(CH_4 \cdots H_2O)$, 23792.77239 $u.a.(CH_4 \cdots CHF_3)$, and 26119.21145 $u.a.(H_2O \cdots CHF_3)$. The tendency of aug-cc-pVTZ to present higher energies is clear and can also be attributed to the higher complexity of this basis set. This pattern can be noted regardless of both the vibrational level and the dimer considered.

We have used the well-established DVR [29] method to compute the spectroscopic constants for our dimers. Table 6 summarizes these results for all dimers, and also provides direct means of comparison between both level aug-cc-pVDZ and aug-cc-pVTZ. In the case of the harmonic constant ω_e the same pattern of aug-cc-pVDZ underestimation is achieved. It could be noted that the harmonic constant ω_e presents a direct relation to the strength of dimers interaction. The more precise level of electronic correlation near equilibrium distance is a possible explanation for the fact that aug-cc-pVTZ presents higher harmonic frequency values. The same feature is not observed, neither for anharmonic constants nor for α_e and γ_e, because for these properties the PEC far from equilibrium distance have small contribution. Experimental microwave spectrum [30] of $CH_4 \cdots H_2O$ shows a stretching frequency of 55 cm^{-1}. Therefore, our value of harmonic frequency, ω_e, is corroborated by this experimental data, mainly for the aug-cc-pVDZ basis set. It must be observed that the experimental result is an average of different conformations, and the theoretical value is from a single conformational state.

The general order found for the decrease of interatomic distances agrees with the increase of D_e (Tables 2 and 3) for all dimers. This suggests that the interaction of $CH_4 \cdots CH_4$ is the weakest among all dimers, followed by $CH_4 \cdots CHF_3$, $CH_4 \cdots H_2O$, and the strongest interaction is of $H_2O \cdots xtitCHF_3$ dimer. The dipole moment (1.85 D for H_2O, 1.65 D for CHF_3 and 0.0 D for CH_4) and electronegativity differences justify this behavior.

The difference between two consecutive rovibrational energies for lower levels has the same trend shown by D_e and R_e. However, for higher levels, the difference for the $CH_4 \cdots H_2O$ and $CH_4 \cdots CHF_3$ approaches the $CH_4 \cdots CH_4$ difference.

Table 6 Rovibrational spectroscopic constants in units of cm^{-1} for $CH_4 \ldots CH_4$, $CH_4 \ldots H_2O$, $CH_4 \ldots CHF_3$, and $H_2O \cdots CHF_3$ dimers

System	Basis set	ω_e	$\omega_e x_e$	$\omega_e y_e$	α_e	γ_e
$CH_4 \ldots CH_4$	aug-cc-pVDZ	47.8391	6.1440	1.62×10^{-1}	1.13×10^{-2}	-9.52×10^{-4}
	aug-cc-pVTZ	52.9765	6.2313	1.20×10^{-1}	1.06×10^{-2}	-1.06×10^{-3}
$CH_4 \ldots H_2O$	aug-cc-pVDZ	68.9563	4.8116	-1.26×10^{-1}	7.89×10^{-3}	-1.21×10^{-3}
	aug-cc-pVTZ	82.6957	5.8483	4.99×10^{-3}	9.89×10^{-3}	-6.08×10^{-3}
$CH_4 \ldots CHF_3$	aug-cc-pVDZ	47.0547	3.5658	3.96×10^{-3}	4.49×10^{-3}	3.68×10^{-4}
	aug-cc-pVTZ	43.6274	–1.1504	-6.58×10^{-1}	5.75×10^{-3}	-1.09×10^{-3}
	aug-cc-pVDZ	93.5787	1.0712	-9.81×10^{-2}	1.41×10^{-3}	-1.47×10^{-4}
	aug-cc-pVTZ	108.1093	3.8416	8.21×10^{-2}	3.11×10^{-3}	-2.32×10^{-5}

Meanwhile, $H_2O\cdots CHF_3$ keeps a large difference from the whole set. Therefore, in the dissociation region of PEC, the attractive forces are still large for $H_2O\cdots CHF_3$. Differently, for $CH_4\cdots H_2$ O and $CH_4 tsCHF_3$ the contribution of repulsive forces increases and becomes similar to $CH_4\cdots CH_4$.

Conclusions

In this work, we performed an extensive study on potential energy curves, spectroscopic constants, and rovibrational spectra of the $CH_4\cdots CH_4$, $CH_4\cdots H_2$ O, $CH_4\cdots CHF_3$, and $H_2O\cdots CHF_3$ dimers. To the best of our knowledge, this is the first time the spectroscopic constants of these dimers have been reported. From total electronic density difference MP2-HF at aug-cc-pVTZ level, it was possible to verify an increase of electron density along the H ⋯ C intermolecular bond for $CH_4\cdots CH_4$ dimer, which suggests that this dimer has been stabilized by dispersion interactions. The same pattern was observed for the other dimers, but in smaller proportions. The ω_e vibrational frequency constant calculations showed that the $H_2O\cdots CHF_3$ frequency is the most harmonic of all studied dimers. Results obtained in this work are of potential use for comparison in future theoretical and experimental works in the spectroscopy and molecular dynamic of the $CH_4\cdots CH_4$, $CH_4\cdots H_2$ O, $CH_4\cdots CHF_3$, and $H_2O\cdots CHF_3$ dimers.

Acknowledgments

The authors gratefully acknowledge the financial support from the Brazilian Research Councils CNPq, CAPES, FAPDF, and FINATEC.

References

1. Vondrasek J, Bendova L, Klusak V, Hobza P (2005) J Am Chem Soc 127:2615–2619
2. Berka K, Laskowski R, Riley KE, Hobza P, Vondrasek J (2009) J Chem Theory Comput 5:982–992
3. Chao SD, Li AHT (2007) J Phys Chem A 111:9586–9590
4. Alkorta I, Maluendes S (1995) J Phys Chem 99:6457–6460
5. Granatier J, Pitonk M, Hobza P (2012) J Chem Theory Comput 8: 2282–2292
6. Alberti M, Aguilar A, Lucas JM, Pirani F (2012) J Phys Chem A 116: 5480–5490
7. Li AHT, Chao SD (2006) J Chem Phys 125:094312
8. Takeuchi H (2012) Comp Theor Chem 986:48–56
9. Grechko M, Aseev O, Rizzo TR, Zobov NF, Lodi L, Tennyson J, Polyansky OL, Boyarkin OV (2012) J Chem Phys 136:244308
10. Yurchenko SN, Carvajal M, Thiel W, Jensen P (2006) J Mol Spect 239:71–87
11. Reid BP, O'Loughlin MJ, Sparks RK (1985) J Chem Phys 83:5656–5662
12. Borysow A, Frommhold L (1987) Astrophys J 318:940–953
13. Mckay CP, Pollack JB, Courting R (1991) Science 253:1118–1121
14. Buryak IA, Kalugina YN, Vigasin AA (2013) J Mol Spectrosc 291: 102–107
15. Boswell R, Collett TS (2011) Energ Environ Sci 4:1206–1215
16. Martins JBL, Politi JRS, Garcia E, Vilela AFA, Gargano R (2009) J Phys Chem A 113:14818–14823
17. Frisch MJ, Trucks GW, Schlegel HB, Scuseria GE, Robb MA, Cheeseman JR, Scalmani G, Barone V, Mennucci B, Petersson GA, Nakatsuji H, Caricato M, Li X, Hratchian HP, Izmaylov AF, Bloino J, Zheng G, Sonnenberg JL, Hada M, Ehara M, Toyota K, Fukuda R, Hasegawa J, Ishida M, Nakajima T, Honda Y, Kitao O, Nakai H, Vreven T, Montgomery JA, Peralta JE, Ogliaro F, Bearpark M, Heyd JJ, Brothers E, Kudin KN, Staroverov VN, Kobayashi R, Normand J, Raghavachari K, Rendell A, Burant JC, Iyengar SS, Tomasi J, Cossi M, Rega N, Millam JM, Klene M, Knox JE, Cross JB, Bakken V, Adamo C, Jaramillo J, Gomperts R, Stratmann RE, Yazyev O, Austin AJ, Cammi R, Pomelli C, Ochterski JW, Martin RL, Morokuma K, Zakrzewski VG, Voth GA, Salvador P, Dannenberg JJ, Dapprich S, Daniels AD, Farkas O, Foresman JB, Ortiz JV, Cioslowski J, Fox DJ (2009) Gaussian 09, Revision A.02. Gaussian, Inc, Wallingford
18. Press WH, Flamery BF, Teukolsky SA, Vetterling WT (1992) Numerical Recipes in Fortran 77. Cambridge Univ Press, New York
19. Neto JJS, Costa LSB (1998) J Phys 28:111
20. Yamamoto T, Kataoka Y, Okada K (1977) J Chem Phys 66:2701
21. Dore L, Cohen RC, Schmuttenmaer CA, Busarow KL, Elrod MJ, Loeser GJ, Saykally RJ (1994) J Chem Phys 100:863–876
22. Akin-Ojo O, Szalewicz K (2005) J Chem Phys 123:134311–134319
23. Rezac J, Simova L, Hobza P (2013) J Chem Theory Comput 9:364–369
24. Copeland KL, Tschumper GS (2012) J Chem Theory Comput 8: 1646–1656
25. Liu Y, Zhao J, Li F, Chen Z (2013) J Comp Chem 34:121–131
26. Rosenberg RE (2012) J Phys Chem A 116:10842–10849
27. Guarini E, Sampoli M, Venturi G, Bafile U, Barocchi F (2007) Phys Rev Lett 99:167801
28. Bagno A, Saielli G, Scorrano G (2002) Chem Eur J 8:2047–255
29. Bramley MJ, Carrington T (1993) J Chem Phys 99:8519–8541
30. Suenran RD, Fraser GT, Lovas FJ, Kawashima Y (1994) J Chem Phys 101:7230